

KINETICS, EQUILIBRIUM AND THERMODYNAMICS OF CONGO RED REMOVAL BY CATIONIZED CELLULOSE OBTAINED FROM CEREAL BY-PRODUCTS

PAUNKA S. VASSILEVA, IVAN M. UZUNOV and DIMITRINKA K. VOYKOVA

*Institute of General and Inorganic Chemistry, Bulgarian Academy of Sciences,
Acad. G. Bonchev Str., 111113 Sofia, Bulgaria*

✉ *Corresponding author: P. S. Vassileva, pnovachka@svr.igic.bas.bg*

Received May 3, 2022

The present study deals with the removal efficiency towards Congo red dye of two cationized cellulose adsorbents prepared from cereal by-products. Rice and einkorn husks were used as raw materials to extract and separate the cellulose by alkali and bleaching treatments. The cellulose materials were modified with N,N-dimethyl-1-octadecylamine to prepare cationized adsorbents. Instrumental methods, such as XRD, DTA, FTIR and SEM, as well as low-temperature nitrogen adsorption, were used for their characterization. The results showed that the quaternary ammonium group was successfully grafted onto the cellulose structures. The survey mainly focused on the effect of process parameters on the adsorption capacity of the investigated materials, including contact time, initial Congo red concentrations, solution pH and temperature. The adsorption process was well described by the pseudo-second-order and Langmuir models. The values of entropy, enthalpy and Gibbs free energy for the Congo red removal were determined.

Keywords: Congo red, rice husks, einkorn husks, adsorption, cereal by-products, cellulose

INTRODUCTION

Many industries, such as textiles, food, leather, paper, printing, pharmaceutical, cosmetics *etc.*, generate considerable amounts of dye-bearing effluents during their production processes.¹ These coloured compounds inhibit sunlight penetration into the stream and affect the aquatic ecosystem. Dyes usually have complex aromatic molecular structures, making them more stable and difficult to biodegrade. Most of these dyes represent a serious hazard to the ecological system as they are considered toxic and have carcinogenic properties. Therefore, dye removal from the environment is an important and challenging area in wastewater treatment. Various conventional methods of removing dyes include flotation, chemical coagulation, chemical oxidation, membrane separation, *etc.*^{1,2} However, these methods are not widely used because of their economic disadvantages. In contrast, adsorption has become one of the most effective methods to remove coloured organic species from contaminated wastewater. The high costs of

commercial adsorbents and losses during regeneration make their use limited. This stimulated the interest in using low-cost natural materials for adsorbents. Many researchers have reported the feasibility of various adsorbents derived from natural materials, industrial solid wastes and agricultural by-products.³⁻⁶

Agricultural residues, such as cereal grain husk, a by-product of the milling industry, are regularly produced on large scale as waste. Therefore, they should be properly utilized for the production of high-value-added products. A possible application of agricultural wastes is as biosorbents, directly or after activation and modification. The internal surface area and availability of different surface functional groups that could play the role of adsorption sites promote the possibility to use lignocellulosic materials as adsorbents from aqueous solutions.^{7,8} Their application has received much attention in the sorption of various pollutants.^{5,6,9} Amongst the variety of agricultural wastes or biomasses available, rice

husks (RH) occupy a prominent position, not only in terms of the amount produced worldwide, but also due to their unique chemistry-related features. Einkorn is one of the oldest cultivated crops in human history. There has been increased interest in recent years in using it as a healthy alternative to wheat, due to its very low gluten and high micronutrient content.¹⁰ The granular structure of the rice and einkorn husks, their phase composition, chemical stability, water resistance and high mechanical strength render them suitable for preparing valuable and inexpensive natural sorbents.^{9,11}

One of the main polysaccharides in plants is cellulose. This natural polymer is an affordable and ecological resource. In plants, cellulose, hemicelluloses, lignin and other concomitants are contained in the cell membrane. The membrane of annual plant species, such as rice and einkorn, is made up of almost pure cellulose. A lot of published results show that cellulose can adsorb different organic and inorganic pollutants from water media. Natural cellulose is made up of glucose units connected by β -(1-4)-glycosidic bonds. A large number of hydroxyl groups in cellulose determines its affinity to oils, fats and dyes. Many researchers have modified cellulose through different processes, such as esterification, graft copolymerization, *etc.* to increase its adsorption ability.^{6,12} Such an approach, together with the above-mentioned advantages of cellulose, has drawn many scientists toward its use as an adsorbent for dye removal.

Cationized cellulose is prepared by grafting cationic functional groups onto the cellulose hydroxyl groups. The modified material acts as an anion exchanger at different pH values, which facilitates the adsorption of anionic contaminants from aqueous solutions by electrostatic attraction. The methods of cationization comprise the embedding of amine or quaternary ammonium groups into the cellulose structure.^{6,13,14}

Congo red (CR) is a synthetic anionic diazo dye that has been used in the textile, paper, printing, leather and plastic industries.¹⁵ It is a significant hazard to aquatic living organisms and a human carcinogen.^{3,15} CR irritates eyes and skin as its main side effect. The structural stability of Congo red is a major challenge for its removal from wastewater.¹³ CR is very sensitive to acids and its colour turns blue in the

presence of acids (below pH 5). The colour variations may be attributed to resonance among charged canonical structures or the protonation of its amino groups.³ In recent years, different adsorbents have been explored for CR removal.^{1,3,4,6,13,15-18}

The present study investigated the synthesis of cationic-modified materials based on rice and einkorn husks and their use for the adsorptive removal of Congo red. The kinetics and thermodynamics of the sorption process were also studied.

EXPERIMENTAL

Materials and chemicals

Rice husks (denoted as RH), from the harvest of 2019, Pazardzhik region, Bulgaria, were used. Einkorn wheat husks (denoted as EH) were collected from the region of Haskovo, Bulgaria.

N,N-dimethyl-1-octadecylamine was purchased from Acros Organics (Belgium). All other reagents used (NaClO_2 , NaHSO_3 , NaOH , epichlorohydrin *etc.*) were analytical grade reagents. Congo red (CAS Number: 573-58-0; PubChem CID: 11313) was purchased from Fisher Chemical (USA). A stock solution of CR dye, containing 1200 mg L^{-1} was prepared by dissolving the required amount of dye powder in deionized water. The pH of the Congo red solution is 6.7 and does not deviate much with dilution. The red colour is stable in the pH range of 5–12.¹⁸ All working solutions of the desired concentrations were prepared by diluting the stock solution with deionized water.

Preparation of cationized materials

The husks, prewashed with deionized water and dried at $120 \text{ }^\circ\text{C}$, were milled on a rotary mill. The sieve fraction with a particle size of less than 0.63 mm was used. The cationic-modified cellulose materials were prepared according to the method proposed by Jiang and Hu.⁶

To remove hemicelluloses and lignin, 50 g of milled rice husks and einkorn husks taken separately were soaked in 1 L of solution containing 40 g of NaOH and 2 g of NaHSO_3 . The suspension was stirred at $90 \text{ }^\circ\text{C}$ for 3 hours, washed with deionized water and dried in a vacuum oven at $60 \text{ }^\circ\text{C}$ for 24 hours. Then, 35 g of products were placed into 1 L of mixed solution comprising 10 g of NaClO_2 and 5 g of acetic acid, and stirred at $70 \text{ }^\circ\text{C}$ for 3 hours to remove the remaining lignin and hemicelluloses. This bleaching treatment breaks down the phenolic compounds and chromophore groups present in the lignin molecule, thus whitening the cellulose samples. Finally, the obtained cellulose materials (denoted as RHC from rice husks and EHC from einkorn husks) were dried in a vacuum at $60 \text{ }^\circ\text{C}$ for 24 hours and milled on a rotary mill to a powder with

a particle size of less than 0.63 mm. Then, the prepared samples (10 g) were mixed with 250 mL of 20% NaOH solution and agitated in an ultrasonic processor (750 Watt) at room temperature for 2 hours. After filtration, the solid phase was treated with 250 mL of 10% NaOH and 240 mL of epichlorohydrin, under agitation for 6 hours at 65 °C. After washing, the precipitates were added to 200 mL of 40% solution of N,N-dimethyl-1-octadecylamine in isopropanol and stirred for 3 hours at 80 °C. The residues obtained after filtration were washed with ethanol, 0.1 M NaOH and HCl, and finally with deionized water. The samples were dried at 60 °C. The synthesized cationic materials were denoted as RHCC, corresponding to rice husks, and EHCC, corresponding to einkorn husks, respectively.

Characterization

The process of modification of the cellulose materials was investigated by thermal analysis, XRD, FTIR and nitrogen low-temperature adsorption.

The thermal behaviour of the samples was determined by complex thermal analysis (TG/DTA). The measurement was performed on a SETARAM *Labsys Evo* 1600 system up to 1000 °C at a heating rate of 10 °C min⁻¹, in an oxygen atmosphere, in an open corundum crucible.

The changes in phase composition were determined by XRD analysis. The patterns were recorded on a D8 Advance System from Bruker Inc. (Germany) (40 kV and 40 mA), using CuK α radiation ($\lambda = 1.5404$ nm).

The available surface functional groups of the samples were investigated by FTIR. The infrared spectra were recorded on a Bruker IFS 25 Fourier transform spectrometer (Germany), in KBr pellets, at a spectral resolution of 2 cm⁻¹ and with an accumulation of 64 scans. The spectra were scanned in the range of 4000–400 cm⁻¹. For the preparation of the KBr pellets, 0.0250 g of the sample was ground in an agate mortar with 1.500 g KBr and then 0.3000 g of the mixture was used to prepare the KBr pellet with a diameter of 13 mm.

The porosity of the samples was determined by nitrogen adsorption/desorption isotherms at -196 °C. The analysis was done on a Quantachrome NOVA 1200e automatic instrument (Quantachrome Instrument Co., USA).

The changes in the morphology of the husks as a result of the treatment procedures were observed by scanning electron microscopy, using a JEOL JSM 6390 microscope, in secondary electron imaging mode (SEI), applying the appropriate magnification.

Adsorption studies

The adsorption of CR was carried out at 20 °C in batch mode experiments. The experiments were carried out in plugged 50 mL Erlenmeyer flasks, containing about 0.2 g of the investigated sample and

20 mL of an aqueous solution of CR. The suspensions were shaken on a rotary shaker at 150 rpm. On reaching equilibrium, the solid particles were separated by centrifuging. Initial and equilibrium CR concentrations were determined spectrophotometrically on a Spekol 11 apparatus (Carl Zeiss Industrielle Messtechnik GmbH) by measuring absorbance at λ_{max} of 420 nm. A blank test was prepared for each sample by mixing all of the reagents in the corresponding sample without CR.

The adsorbed amount at equilibrium (Q_e , mg/g) was calculated using the equation:

$$Q_e = (C_0 - C_e) * V/m \quad (1)$$

where C_0 and C_e are the initial and equilibrium concentration of CR (mg L⁻¹), respectively; V is the solution volume (L) and m is the sorbent mass (g). Each experiment was performed in triplicate.

To optimize contact time for CR adsorption, kinetic experiments were carried out. The adsorption was investigated at different time intervals, from 5 min to 2 hours. Kinetic adsorption experiments were performed using solutions with initial ion concentrations of 500 mg L⁻¹. The effect of initial CR concentrations was studied in the range of 200–1200 mg L⁻¹.

RESULTS AND DISCUSSION

Characterization of the samples

Thermal analysis

The TG/DTA results are presented in Figure 1. The moisture content, the quantity of volatile matter and ash residue of the tested samples are listed in Table 1.

The strong sharp peak, observed in the temperature interval 230–360 °C for all the samples is due to the thermal degradation of cellulose and hemicelluloses.^{19,21} The process is exothermic and takes place by the cleavage of β (1-4) glycoside bonds of cellulose.²² The volatile matter of hemicellulose degradation includes CO_x, H₂O, acetic acid, furfural *etc.*²³ The second exothermic peak, observed for samples RH and EH in the temperature interval 370°–450° C is associated with the thermal degradation of lignin. The main volatile products released are coniferyl aldehyde, coniferyl alcohol, 4-vinyl guaiacol, vanillin, *etc.*^{24,25} For the RHC and EHC samples, this peak is absent, which is an indication of complete lignin extraction as a result of the treatment of the husks with NaOH and NaHSO₃ solution. As can be seen from the data in Table 1, the amount of volatile substances decreases. The predominant phase in the ash residue is amorphous silica.^{26,27} The content of inorganic

impurities in both samples increased at the expense of the extracted lignin and hemicelluloses. Part of the ash content is extracted by the alkaline solution in the form of soluble sodium metasilicate. This process also

leads to changes in the surface morphology of the samples.

Table 1
Characteristics of the husks before and after lignin/hemicellulose removal

Sample	Moisture content (wt%)	Volatile matter (wt%)	Ash residue (wt%)
RH	6.4	72.1	21.5
EH	7.6	84.3	8.1
RHC	5.7	68.2	26.1
EHC	1.8	77.4	20.8

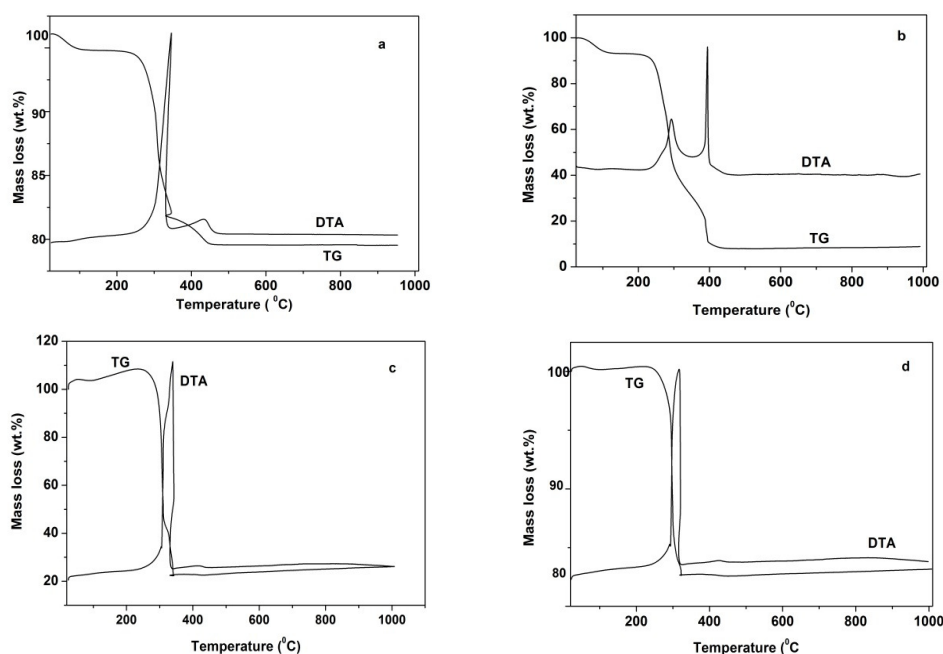


Figure 1: Thermal analysis of RH (a); EH (b); RHC (c) and EHC (d)

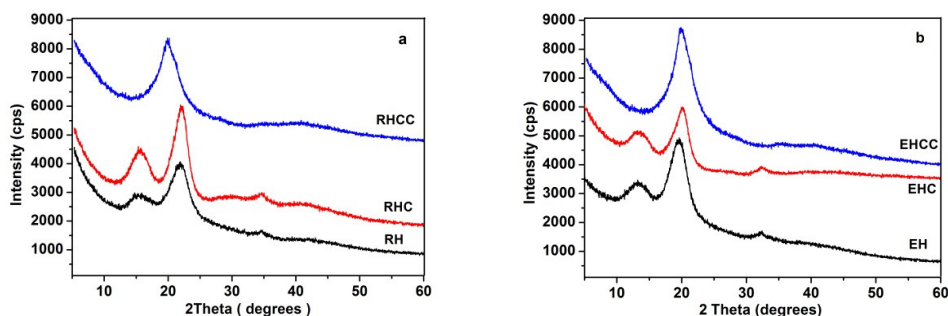


Figure 2: XRD analysis of RH, RHC and RHCC (a); and EH, EHC and EHCC (b)

XRD analysis

The diffraction patterns of the two samples are represented in Figure 2 (a,b). For rice husks and

einkorn husks, before and after bleaching (samples RHC and EHC), the crystallization peaks typical of cellulose are observed at $2\theta =$

15.7°, 22.2° and 34.5°, respectively.²⁸⁻³⁰ After processing the cellulose with N,N-dimethyl-1-octadecylamine, these peaks disappeared and a new peak is registered at $2\theta = 20^\circ$. The alkali treatment and the introduction of amino groups lead to the partial destruction of the crystalline structure of the cellulose. A replacement process of the hydroxyl groups in the cellulose molecule takes place. It is associated with the rupture of hydrogen bonds, as well as with the destruction of the molecular chain.

FTIR analysis

The spectra of the raw rice husks and einkorn husks, as well as those of RHC and EHC samples, are shown in Figure 3. The IR spectra of the raw husks are typical of lignocellulosic materials, which also contain a high amount of inorganic admixtures.^{31,32} There is an overlap of the characteristic absorption bands of lignin, cellulose and hemicelluloses.³³ As can be seen, the spectrum of raw rice husks is dominated by the characteristic bands of cellulose and hemicelluloses, whereas that of einkorn husks is dominated by those of lignin. The spectra of both samples, after bleaching, showed the absence of lignin and hemicelluloses. These are typical IR spectra of cellulose. The following characteristic bands are observed in the EHC

sample: at 3400 cm^{-1} – due to hydroxyl groups (OH stretching), 2900 cm^{-1} (C-H asymmetric stretching vibration of the $-\text{CH}_2-$ groups); 1650 cm^{-1} and 1431 cm^{-1} (asymmetric and symmetric stretching vibration of C-O groups); 1165 cm^{-1} and 1115 cm^{-1} (C-O-C stretching in the glucose structure); 1064 cm^{-1} (C-O stretching and deformation) and 617 cm^{-1} due to C-C stretching vibrations.^{29,33} Additional bands in the spectrum of the RHC sample are those at 1734 cm^{-1} and 1515 cm^{-1} , attributed to C=O stretching, and that observed at 1463 cm^{-1} , due to the (O-CH₃) group. The modification leads to changes in the IR spectra of the two cellulosic materials. The appearance of the two new bands, typical of N,N-dimethyl-1-octadecylamine at 2922 cm^{-1} and 2853 cm^{-1} , is an indication of its incorporation into the cellulose structure. In addition, in the EHC sample, a shift of the band associated with the symmetric stretching vibration of C-O groups from 1431 cm^{-1} to 1463 cm^{-1} , as well as the appearance of a new peak at 1420 cm^{-1} , was observed. The peak at 1165 cm^{-1} , associated with C-O-C stretching vibration, shifts to 1158 cm^{-1} .

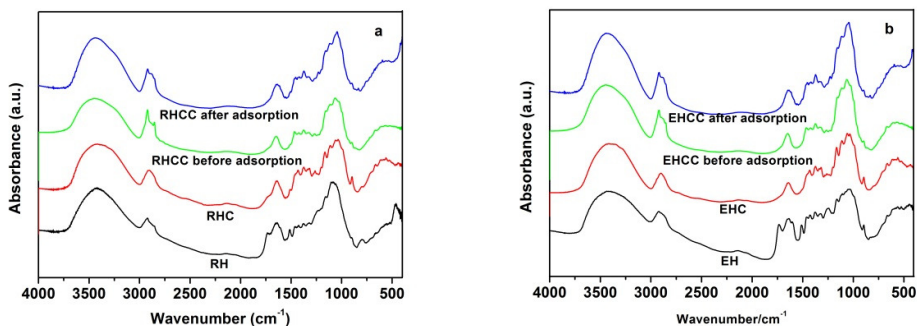


Figure 3: FTIR spectra of RH, RHC, RHCC, RHCC after CR adsorption (a) and EH, EHC, EHCC, EHCC after CR adsorption (b)

The results reveal that dimethyl octadecyl amine was successfully grafted onto the cellulose structure.

In Figure 3, the IR spectra of sorbents RHCC and EHCC, before and after CR adsorption, are also presented. The interaction between the dye molecules and the different functional groups on RHCC and EHCC is supposed to induce some changes in the spectra after the sorption process. The spectra show band shifting and possible involvement of hydroxyl groups around the broad peak at 3400 cm^{-1} . Little changes are

noticed in the asymmetric C=O band in the region of $1640\text{--}1650\text{ cm}^{-1}$, indicating possible carboxyl binding. A new band appears at 1456 cm^{-1} , which can be attributed to the stretching vibration of the C-N group from CR.³⁴ The changes in the bands in the region of $1115\text{--}1040\text{ cm}^{-1}$ prove the participation of the C-O-C and C-O structure in the adsorption process. The band at 617 cm^{-1} characteristic of both samples also shifted to 596 cm^{-1} . From the spectra, it appears that carboxyl, hydroxyl groups and C-O and C-O-C groups are involved in CR binding onto the

investigated adsorbents, as has been also pointed out by Munagapati and Kim.¹³

SEM observation

Figure 4 represents the SEM micrographs at different magnifications of raw rice and einkorn husks; the bleached husks and those treated with N,N-dimethyl-1-octadecylamine. After the

treatment of the husks with NaOH and Na₂HSO₃ at high temperatures, the destruction of the typical corrugated structure of the husks is observed. It is due to the removal of the lignin and hemicelluloses. The process of modification leads to drastic changes in the surface morphology of both samples, as can be seen in Figure 4 (g-j).

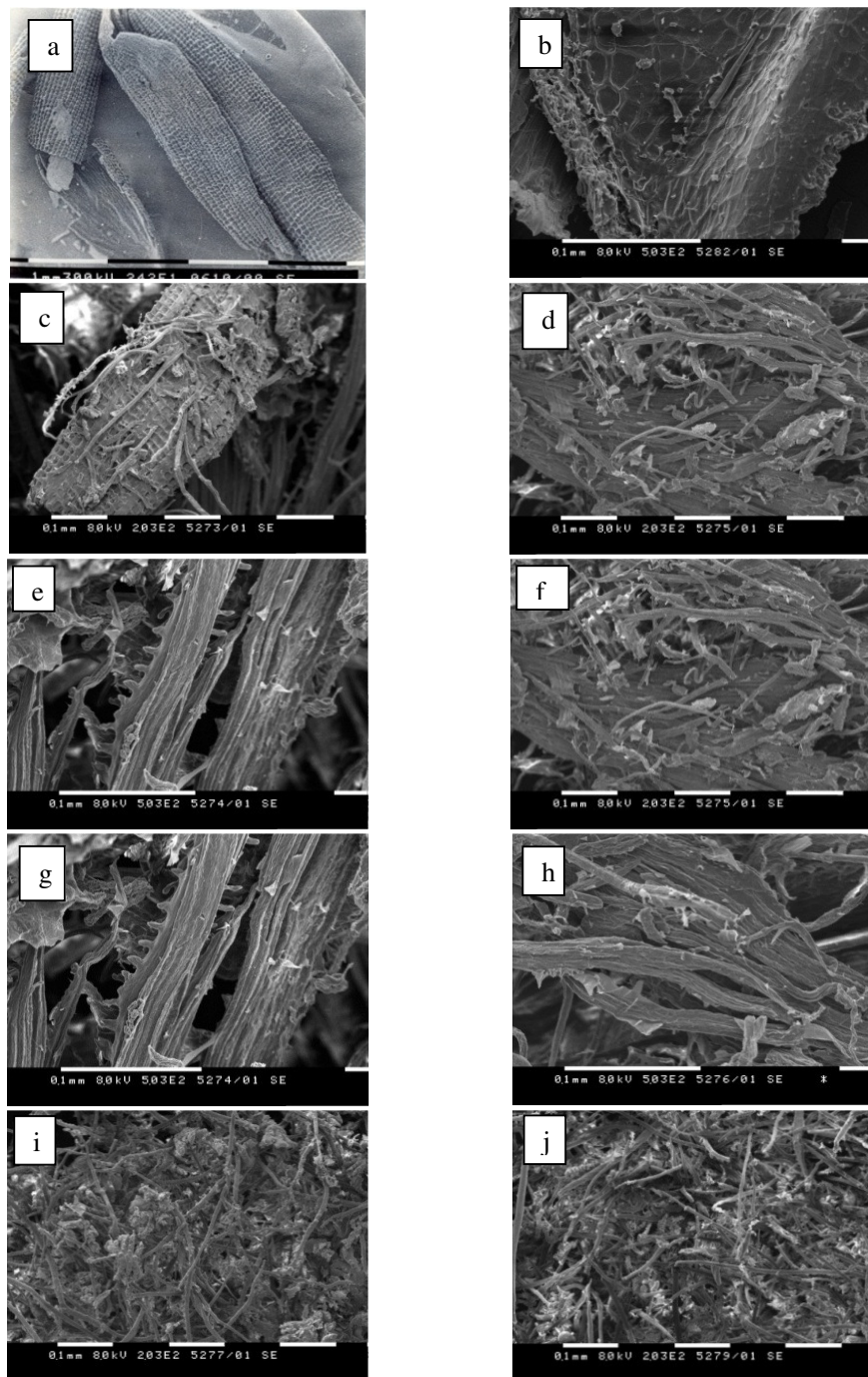


Figure 4: SEM micrographs of RH and EH (a, b); RHC and EHC (c-f); RHCC and RHCC (g-j)

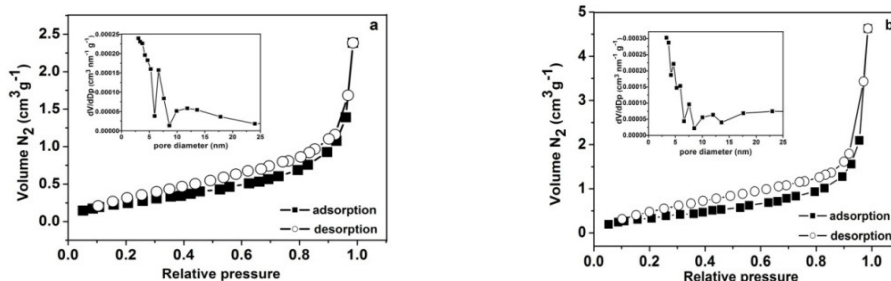


Figure 5: Nitrogen adsorption-desorption isotherms and pore size distribution of the RHCC (a) and EHCC (b)

As can be seen, a rod-shaped structure is formed as a result of the polymer molecular chain destruction.

Porosity

The nitrogen adsorption-desorption isotherms and the pore size distribution of cationized materials are presented in Figure 5. Both presented isotherms belong to type IV, with a hysteresis loop that resembles the H3 type in the IUPAC classification. This hysteresis pattern can be attributed to the crystalline agglomerates that result in the mesoporous structure formed by the interparticle space that causes the formation of secondary pores.²⁶ The specific surfaces and total pore volumes for the materials are as follows: specific surface area – 0.5 m² g⁻¹ and 0.6 m² g⁻¹; and total pore volumes – 0.002 cm³ g⁻¹ and 0.004 cm³ g⁻¹ for sample RHCC and sample EHCC, respectively. Both samples present broad pore size distributions and the mesopores are dominant. The calculated average pore diameters are 31 nm for RHCC and 13 nm for EHCC, which correspond to a mesoporous structure.

Adsorption studies

Effect of pH on the adsorption process

The pH of the aqueous solution is an important parameter that controls the electrostatic interactions between the adsorbent and the adsorbate. The effect of the pH of the initial solution on CR adsorption onto the investigated materials is illustrated in Figure 6. The pH of the CR solution varied from 5.0 to 11.5, because the red colour is stable in the pH range of 5–12, and the colour solution would turn blue at a pH below 5.0.¹⁸ It is seen that the adsorption onto both sorbents slightly decreased as the pH value increased. The optimum pH

value was found to be about 7 (6.7 was the initial pH value of the Congo red solutions).

The anionic dye CR forms negatively charged ions in aqueous media. The high adsorption capacity observed at low pH values was probably due to the strong electrostatic attraction between the positive charges of the adsorbents surface and CR molecules.³ At high pH values, the adsorption of CR decreases because of a reduction in electrostatic attraction as a consequence of the protonation of functional groups of the sorbents and as a result of the competition between increasing OH ions and dye molecules.^{3,35}

Effect of contact time

The adsorbed amount of CR was found to increase with the increase in agitation time and reached a maximum value within 10 min for both materials. At longer contact times, the amount of adsorbed CR remained unchanged. This suggests an excellent affinity of the investigated sorbents towards CR. Nevertheless, all further experiments were performed at a contact time of 2 hours.

The adsorption mechanism can be demonstrated with the help of several models. To investigate the mechanism of adsorption, three kinetic models: pseudo-first-order, pseudo-second-order and intraparticle diffusion were applied to analyse the experimental data:

$$\log(Q_e - Q_t) = \log(Q_e) - (k_1/2.303) t \quad (2)$$

$$(t/Q_t) = (1/k_2 Q_e) + (1/Q_e) t \quad (3)$$

$$Q_t = k_{id} t^{1/2} + C \quad (4)$$

where Q_t is the adsorbed amount of CR for a certain time t (mg g⁻¹) and k_1 is the rate constant of pseudo-first-order adsorption (h⁻¹); Q_e is the equilibrium adsorption capacity (mg g⁻¹) and k_2 is the rate constant of pseudo-second-order adsorption (g mg⁻¹h⁻¹); k_{id} is the intraparticle

diffusion rate constant ($\text{mg g}^{-1}\text{h}^{-1/2}$). The k_1 values were calculated from the slope of the plots $\log(Q_e - Q_t)$ vs. t ; k_2 values were calculated from the slope of the plots t/Q_t vs. t ; k_{id} – were calculated from the slope of the plots Q_t versus $t^{1/2}$. The intercepts of these curves were used to determine the equilibrium capacity (Q_e and C). The model parameters and their statistics are presented in Table 2.

The kinetics of CR adsorption onto both materials is close to the second-order model. The correlation coefficients calculated for

RHCC and EHCC were closer to unity. The predicted equilibrium capacities for the pseudo-second-order model for both biomaterials have a good correlation with the experimental values of Q_e . The results revealed that CR adsorption is adequately described by the pseudo-second-order kinetic equation. This means that the speed of the process depends on the dye concentration in the solution, as well as on the number of adsorption sites on the adsorbent surfaces.³⁶

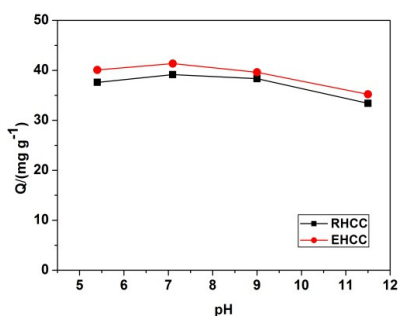


Figure 6: Effect of pH on CR adsorption by RHCC and EHCC

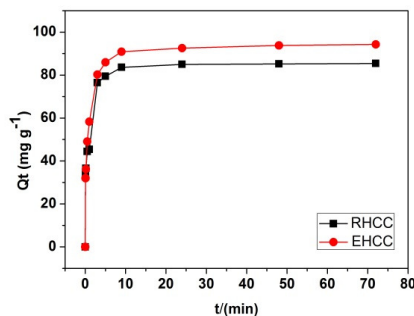


Figure 7: Effect of contact time on CR adsorption onto RHCC and EHCC

Table 2
Kinetic parameters for CR adsorption

Sample	Pseudo-first order constants	Pseudo-second order constants	Intraparticle diffusion constants
	$Q_e k_1 r^2$ (mg g^{-1}) (h^{-1})	$Q_e k_2 r^2$ (mg g^{-1}) ($\text{g mg}^{-1} \text{h}^{-1}$)	$k_{id} C r^2$ ($\text{mg g}^{-1} \text{h}^{1/2}$) (mg g^{-1})
RHCC	22.36 0.022 0.8855	85.91 2.62 0.9999	3.805 30.14 0.9517 1.118 77.43 0.8148
EHCC	28.66 0.018 0.9031	94.77 2.27 0.9999	3.768 21.24 0.9978 1.688 81.94 0.8369

To evaluate the role of diffusion as a process determining the rate of CR adsorption on RHCC and EHCC, the diffusion kinetic equation given by Weber and Morris was also used. The obtained results show that the adsorption process takes place in several stages. In the kinetic graph, two linear regions are observed. It proved that diffusion is not a rate-determining process during CR adsorption in this case.

Adsorption isotherms

Experimental adsorption isotherms for the studied materials are presented in Figure 8. The equilibrium adsorption isotherm gives information regarding the way the adsorbate molecules or ions are distributed between the

solid adsorbent and the solution. In the present research, the adsorption equilibrium data of CR were analysed using three of the most widely used isotherm models – Langmuir, Freundlich and Dubinin-Radushkevich models. The linear form of the Langmuir isotherm is expressed by the equation:

$$C_e/Q_e = 1/KLQ_0 + C_e/Q_0 \tag{5}$$

where C_e is the concentration of CR in the equilibrium solution (mg L^{-1}); Q_e is the amount of CR adsorbed (mg) per unit mass of adsorbent (g); Q_0 is the maximum adsorption capacity (mg g^{-1}); K_L is the Langmuir constant related to enthalpy of the process.

The linear form of the Freundlich model is expressed by the equation:

$$\ln Q_e = \ln k_F + (1/n) \ln C_e \quad (6)$$

where k_F is a constant related to the adsorption capacity and n is an empirical parameter.

The Dubinin–Radushkevich isotherm reveals the adsorption mechanism based on the potential theory. The linear form of the Dubinin–Radushkevich isotherm is described by the equation:

$$\ln Q_e = \ln Q_m - \beta \varepsilon^2 \quad (7)$$

where Q_e is the amount of CR (mg) adsorbed per unit mass of adsorbent (g); Q_m is the maximum adsorption capacity (mg g^{-1}); β is the adsorption energy constant ($\text{mol}^2 \text{J}^{-2}$), and ε is the Polanyi potential, calculated by Equation 8:

$$\varepsilon = RT \ln(1 + 1/C_e) \quad (8)$$

where R is the universal gas constant ($\text{J mol}^{-1} \text{K}^{-1}$) and T is the temperature (K). The mean adsorption energy E (KJ mol^{-1}) can be calculated using the parameter β by Equation 9:

$$E = 1/(-2\beta)^{1/2} \quad (9)$$

The value of the maximum adsorption capacity for RHCC and EHCC obtained from the experimental determinations are 101.35 and 119.65 mg g^{-1} , respectively. The material based on einkorn husks exhibits slightly higher adsorption capacity. This fact can be explained by the results obtained for texture parameters. The calculated isotherm constants and the

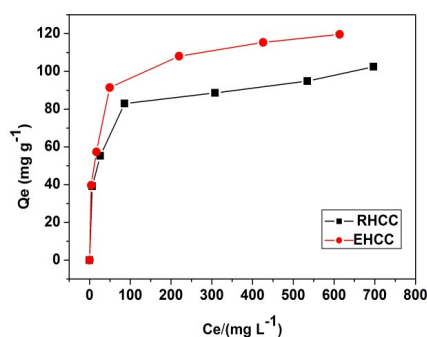


Figure 8: Experimental adsorption isotherms toward CR

The capacity values vary widely for different biosorbents, depending on the experimental conditions. RHCC and EHCC materials display reasonably good adsorption capacities for CR, and could be used as potential adsorbents for effective removal of this dye from polluted waters. Table 4 shows that the modification of the biosorbents leads to an increase in their

correlation coefficients for the three models discussed above are presented in Table 3. As seen, the three isotherm models provide good correlations for CR adsorption. From the values of the correlation coefficients r^2 (greater than 0.998), it is obvious that the Langmuir model most adequately describes the adsorption process for both biomaterials, in the studied concentration range. On the other hand, the values calculated for maximum adsorption capacity according to the Langmuir model were very close to the experimental values. These results indicate mostly homogeneous surface binding and monolayer adsorption. The same result has been reported by other research works.^{3,6,13,15,18}

The n -values in the Freundlich equation are 5.06 and 4.55, respectively, which indicates favourable adsorption onto both materials.^{36,37}

The Dubinin–Radushkevich isotherm model gives information for the adsorption energy. The calculated values for mean free energy for RHCC and EHCC are 0.089 and 0.122 (kJ mol^{-1}), respectively, indicating mainly a physisorption process.

The adsorption capacity of the developed adsorbents was compared with those of other lignocellulosic materials reported in the literature (Table 4).

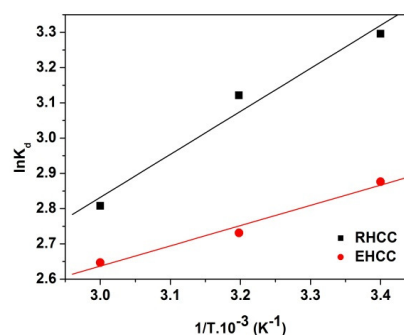


Figure 9: Variation of equilibrium constant as a function of temperature

adsorption capacity towards Congo red. On the other hand, the differences in the adsorption capacity values of the samples observed in the present study can also be explained by the fact that they represent modified cellulose solely and do not contain the functional groups characteristic of lignin and hemicelluloses.

Table 3
Isotherm constants and correlation coefficients for CR adsorption onto RHCC and EHCC

Sample	Langmuir parameters			Freundlich parameters			Dubinin-Radushkevich parameters		
	Q ₀ (mg g ⁻¹)	K ₁ (L mg ⁻¹)	r ²	k _F (mg ¹⁻ⁿ L ⁿ g ⁻¹)	n (L mg ⁻¹)	r ²	Q _{m(o)} (mg g ⁻¹)	E (kJ mol ⁻¹)	r ²
RHCC	102.35	0.042	0.9980	28.96	5.06	0.9719	93.41	0.089	0.9082
EHCC	121.51	0.058	0.9995	31.75	4.55	0.9702	110.72	0.122	0.9247

Table 4
Comparison of maximum adsorption capacities of RHCC and EHCC with those of other lignocellulosic adsorbent materials towards CR

Adsorbent	Adsorption capacity, mg.g ⁻¹	References
Rice husk	1.58	[15]
Modified rice husk	2.04	
Pine bark	3.2	[16]
Banana peel	1.72	[17]
Coir pith	2.8	[38]
Natural celery residues	238.09	
CTAB modified celery residues	526.32	[39]
Stinging nettle	172.14	[40]
Date stones	45.08	
Jujube shells	59.55	[41]
Amino functionalized walnut shells	224.4	[42]
RHCC	102.35	Present
EHCC	121.51	study

Table 5
Values of ΔG^0 , ΔH^0 and ΔS^0 at different temperatures for CR adsorption

Sample	ΔH^0 (kJ mol ⁻¹)	ΔS^0 (J mol ⁻¹ K ⁻¹)	ΔG^0 (kJ mol ⁻¹) 293 K, 313 K, 333 K
	RHCC	-9.54	-8.61
EHCC	-20.29	-41.40	-8.16, -7.33, -6.50

Thermodynamic studies

The effect of temperature on CR adsorption was studied at 20, 40 and 60 °C. The amounts of CR removed by the two biomaterials were found to decrease with increasing temperature. This suggests that the process is exothermic. The decrease in the adsorption efficiency towards the CR dye with increasing temperature is due to the growing tendency for desorption at the interface with the solution.

Changes in the Gibbs free energy (ΔG^0), enthalpy (ΔH^0), and entropy (ΔS^0) were calculated using the following equations:

$$K_d = Q_e / C_e \quad (10)$$

$$\Delta G^0 = -RT \ln K_d \quad (11)$$

$$\ln K_d = \Delta S^0 / R - \Delta H^0 / RT \quad (12)$$

where K_d is the equilibrium constant, R is the gas constant (J mol⁻¹K⁻¹) and T is the temperature (K). The enthalpy change, ΔH^0 , and

the entropy change, ΔS^0 , are determined from the slope and intercept of the plot of $\ln K_d$ versus $1/T$, respectively (Fig. 9). The values of ΔG^0 , ΔH^0 and ΔS^0 parameters are summarized in Table 5.

Changes in the standard free energy have negative values, which indicates that the adsorption of Congo red dye onto RHCC and EHCC is feasible and spontaneous. In addition, physisorption is the dominating mechanism since ΔG^0 values are between 0 and 20 (kJ mol⁻¹).³⁷ The negative values of ΔH^0 proved the exothermic nature of CR adsorption. On the other hand, the obtained values of ΔH^0 confirmed that the adsorption was physical. As a result, the weakening of hydrogen bonds and van der Waals interactions at higher temperatures resulted in the weakening of physical interactions between the active sites of the studied biosorbents and the dye molecules,

decreasing the removal efficiency.¹⁶ The value of ΔH^0 is greater for EHCC than for RHCC. This suggests that adsorption at the surface of EHCC is more spontaneous and exothermic than that of RHCC. Table 5 showed that the values of ΔS^0 for both adsorbents are also negative. The obtained results reveal that the dye molecules have a high degree of freedom and hence their randomness in the bulk of the solution, compared to their attachment to the surface of the adsorbent. It further indicates that the adsorbed molecules become more localized at the solid/water interface, compared to their delocalized Brownian movement in the bulk of the solution.¹⁵

Desorption studies

The regeneration of the sorbent and the disposal of the adsorbate-loaded adsorbent are problems of great importance. Therefore, desorption experiments were also carried out. 0.01 M and 0.1 M NaOH were used for CR desorption. 0.1 M NaOH showed higher recovery efficiency – of 77% for RHCC and 70% for EHCC, compared to 0.01 M NaOH (38% for RHCC and 32% for EHCC, respectively) and is thus considered a suitable eluting agent for the regeneration of both biosorbents. It was observed that the desorption increases with increasing eluent concentration and the corresponding increase in the pH value of the desorbing medium. This shows that the adsorption is dominated by electrostatic interaction and hydrogen bonding.¹⁸

CONCLUSION

Novel cationized cellulose adsorbents based on rice and einkorn husks were synthesized by modification of cellulose materials with N,N-dimethyl-1-octadecylamine. The removal of lignin and hemicelluloses from the plant matrix leads to changes in the surface morphology of the samples, their phase composition, surface functional groups and porous structure. The characterization of cationized materials shows that the quaternary ammonium group was successfully grafted onto the cellulose structures. The adsorption isotherms and kinetics towards Congo red dye were evaluated. The experimental data analysis of CR adsorption revealed the best fit to the pseudo-second-order kinetic model. The material EHCC, based on einkorn husks demonstrated higher CR removal performance, with an

adsorption capacity of 121.51 mg g⁻¹, according to the Langmuir model. The negative values of change in Gibbs free energy and enthalpy change indicate that the adsorption of CR onto the studied materials is spontaneous and exothermic, with a negative entropic change. Based on the experimental results, it can be concluded that these novel cationized cellulose materials can be used as potential adsorbents for the effective removal of CR from contaminated aqueous solutions. 0.1M NaOH solution is a suitable eluting agent for the regeneration of both biosorbents. The obtained results reveal that renewable agriculture wastes can be successfully processed into products with added value and applicability in protecting the environment from hazardous pollutants.

ACKNOWLEDGEMENTS: The research leading to these results received funding from the Bulgarian Ministry of Education and Science under the National Research Programme “Healthy Foods for a Strong Bio-Economy and Quality of Life” approved by DCM # 577/17.08.2018.

REFERENCES

- ¹ A. Bożęcka, M. Orlof-Naturalna and M. Kopeć, *J. Ecol. Eng.*, **22**, 111 (2021), <https://doi.org/10.12911/22998993/141368>
- ² V. Katheresan, J. Kannedo and S. Lau, *J. Environ. Chem. Eng.*, **6**, 4676 (2018), <https://doi.org/10.1016/j.jece.2018.06.060>
- ³ Y. Zhou, L. Ge and N. Fan, *Adsorpt. Sci. Technol.*, **36**, 1310 (2018), <https://doi.org/10.1177/0263617418768945>
- ⁴ T. Taher, D. Rohendi, R. Mohadi and A. Lesbani, *Arab J. Basic Appl. Sci., Univ. Bahrain*, **26**, 125 (2019), <https://doi.org/10.1080/25765299.2019.1576274>
- ⁵ M. Sulyman, J. Namiesnik and A. Gierak, *Pol. J. Environ. Stud.*, **26**, 479 (2017), <https://doi.org/10.15244/pjoes/66769>
- ⁶ Z. Jiang and D. Hu, *J. Mol. Liq.*, **276**, 105 (2019), <https://doi.org/10.1016/j.molliq.2018.11.153>
- ⁷ S. Uzunova, L. Minchev, I. Uzunov and V. Toteva, *Chem. Ecol.*, **32**, 976 (2016), <https://doi.org/10.1080/02757540.2016.1212850>
- ⁸ K. Asemave, L. Thaddeus and P. Tarhamba, *Sustain. Chem.*, **2**, 271 (2021), <https://doi.org/10.3390/suschem2020016>
- ⁹ P. Vassileva, T. Radoykova, A. Detcheva, I. Avramova, K. Aleksieva *et al.*, *Int. J. Environ. Sci. Technol.*, **13**, 1319 (2016), <https://doi.org/10.1007/s13762-016-0970-y>

- ¹⁰ G. Gentsheva, I. Uzunov, I. Karadjova and A. Predoeva, *CR Acad. Bulg. Sci.*, **67**, 647 (2014)
- ¹¹ Z. Shamsollahi and A. Partovinia, *J. Environ. Manag.*, **246**, 314 (2019), <https://doi.org/10.1016/j.jenvman.2019.05.145>
- ¹² S. Hokkanen, A. Bhatnagar and M. Sillanpää, *Water Res.*, **91**, 156 (2016), <https://doi.org/10.1016/j.watres.2016.01.008>
- ¹³ V. Munagapati and D.-S. Kim, *J. Mol. Liq.*, **220**, 540 (2016), <https://doi.org/10.1016/j.molliq.2016.04.119>
- ¹⁴ A. Aly, S. Mahmoud and M. El-Asasery, *Pigment. Resin. Technol.*, **47**, 108 (2018), <https://doi.org/10.1108/PRT-10-2016-0092>
- ¹⁵ A. Malik, A. Khan, N. Anwar and M. Naeem, *Bull. Chem. Soc. Ethiop.*, **34**, 41 (2020), <https://doi.org/10.4314/bcse.v34i1.4>
- ¹⁶ K. Litefti, M. Freire, M. Stitou and J. González-Álvarez, *Sci. Rep.*, **9**, 16530 (2019), <https://doi.org/10.1038/s41598-019-53046-z>
- ¹⁷ N. Mondal and S. Kar, *Appl. Water Sci.*, **8**, 157 (2018), <https://doi.org/10.1007/s13201-018-0811-x>
- ¹⁸ R. Lafi, I. Montasser and A. Hafiane, *Adsorpt. Sci. Technol.*, **37**, 160 (2019), <https://doi.org/10.1177/0263617418819227>
- ¹⁹ H. Yang, R. Yan, H. Chen, D. Lee and C. Zheng, *Fuel*, **86**, 1781 (2007), <https://doi.org/10.1016/j.fuel.2006.12.013>
- ²⁰ P. Aggarwal, D. Dollimore and K. Heon, *J. Therm. Anal.*, **50**, 7 (1997), <https://doi.org/10.1007/BF01979545>
- ²¹ S. Vicini, E. Princi, G. Luciano, E. Franceschi, E. Pedemonte *et al.*, *Thermochim. Acta*, **418**, 123 (2004), <https://doi.org/10.1016/j.tca.2003.11.049>
- ²² Y. Lin, J. Cho and G. Tompsett, *J. Phys. Chem. C*, **113**, 20097 (2009), <https://doi.org/10.1021/jp906702p>
- ²³ S. Wang, B. Ru, H. Lin and Z. Luo, *Bioresour. Technol.*, **143**, 378 (2013), <https://doi.org/10.1016/j.biortech.2013.06.026>
- ²⁴ H. Kawamoto, *J. Wood Sci.*, **63**, 1 (2017), <https://doi.org/10.1007/s10086-016-1606-z>
- ²⁵ P. Patwardhan, R. Brown and B. Shanks, *ChemSusChem*, **4**, 1629 (2011), <https://doi.org/10.1002/cssc.201100133>
- ²⁶ P. Vassileva, A. Detcheva, S. Uzunova, I. Uzunov and D. Voykova, *Separ. Sci. Technol.*, **51**, 797 (2016), <https://doi.org/10.1080/01496395.2015.1136331>
- ²⁷ D. Radev, I. Uzunov, B. Kunev, V. Tumbalev and P. Tsokov, *AIP Conf. Proc.*, **9**, 68 (2009)
- ²⁸ K. Das, D. Ray, N. Bandyopadhyay and S. Sengupta, *J. Polym. Environ.*, **18**, 355 (2010), <https://doi.org/10.1007/s10924-010-0167-2>
- ²⁹ M. Poletto, H. Ornaghi Júnior and A. Zattera, *Materials*, **7**, 6105 (2014), <https://doi.org/10.3390/ma7096105>
- ³⁰ S. Keshk and M. Hamdy, *Turk. J. Chem.*, **43**, 94 (2019), <https://doi.org/10.3906/kim-1803-83>
- ³¹ W. Nakbanpote, B. Goodman and P. Thiravetyan, *Colloid. Surf. A: Physicochem. Eng. Asp.*, **304**, 7 (2007), <https://doi.org/10.1016/j.colsurfa.2007.04.013>
- ³² M. Morcali, B. Zeytuncu and O. Yucel, *Mater. Res.*, **16**, 528 (2013), <https://doi.org/10.1590/S1516-14392013005000006>
- ³³ H. Yang, R. Yan, H. Chen, D. H. Lee and C. Zheng, *Fuel*, **86**, 1781 (2007), <https://doi.org/10.1016/j.fuel.2006.12.013>
- ³⁴ A. Bartošová, L. Blinová, M. Sirotiak and A. Michalíková, *Res. Pap., Fac. Mat. Sci. Technol., Slovak Univ. Technol. Bratisl.*, **25**, 103 (2017), <https://doi.org/10.1515/rput-2017-0012>
- ³⁵ L. Ge, Y. Zhou, N. Fan, M. S. Xia, L. Q. Dai *et al.*, *Desalin. Water Treat.*, **81**, 291 (2017), <https://doi.org/10.5004/dwt.2017.21059>
- ³⁶ P. Vassileva, D. Voykova, I. Uzunov and S. Uzunova, *CR Acad. Bulg. Sci.*, **71**, 1192 (2018), <https://doi.org/10.7546/CRABS.2018.09.05>
- ³⁷ P. Vassileva and D. Voikova, *J. Hazard. Mater.*, **170**, 948 (2009), <https://doi.org/10.1016/j.jhazmat.2009.05.062>
- ³⁸ Ü. Geçgel and H. Kolancıla, *Nat. Prod. Res.*, **26**, 659 (2012), <https://doi.org/10.1080/14786419.2010.541878>
- ³⁹ S. Mohebali, D. Bastani and H. Shayesteh, *J. Mol. Struct.*, **1176**, 181 (2019), <https://doi.org/10.1016/j.molstruc.2018.08.068>
- ⁴⁰ B. Ertan, *Cellulose Chem. Technol.*, **55**, 1131 (2021), <https://doi.org/10.35812/CelluloseChemTechnol.2021.55.97>
- ⁴¹ N. El Messaoudi, A. Dbik, M. El Khomri, A. Sabour, S. Bentahar *et al.*, *Int. J. Phytoremediat.*, **19**, 1047 (2017), <https://doi.org/10.1080/15226514.2017.1319331>
- ⁴² E. Dovi, A. Aryee, A. Kani, F. M. Mpatani, J. Li *et al.*, *J. Environ. Chem. Eng.*, **9**, 106301 (2021), <https://doi.org/10.1016/j.jece.2021.106301>